Marine Chemistry 197 (2017) 64–69

Contents lists available at ScienceDirect

Marine Chemistry

journal homepage: www.elsevier.com/locate/marchem

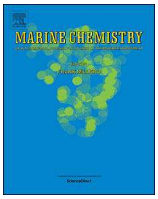

Spectrophotometric pH measurements from river to sea: Calibration of mCP for $0 \leq S \leq 40$ and $278.15 \leq T \leq 308.15$ K

N.K. Douglas, R.H. Byrne*

College of Marine Science, University of South Florida, 140 7th Avenue South, St. Petersburg, FL 37701, USA

ARTICLE INFO

Keywords:
m-Cresol Purple
Spectrophotometry
Estuary
Freshwater
pH

ABSTRACT

The indicator meta-cresol purple (mCP) has been widely used for spectrophotometric pH measurements in seawater and has been recently used in freshwater as well. Previous works have not, however, provided the comprehensive characterization of purified mCP (equilibrium and spectral behavior) required for pH measurements across the full ranges of temperature (T) and salinity (S) found in temperate estuaries. This work provides, for the first time, a comprehensive S- and T-dependent model for spectrophotometric pH measurements appropriate to freshwater, estuarine water, and seawater. Our model combines previous characterizations of the behavior of (a) purified mCP in pure water ($S = 0$), (b) purified mCP in seawater ($20 \leq S \leq 40$), and (c) unpurified mCP at 298.15 K and $0 \leq S \leq 40$, herein corrected for the effects of impurities. Using the ratio (R) of mCP absorbances at 578 nm and 434 nm, the summary equations for calculations of pH on the total proton concentration scale for the conditions of $0 \leq S \leq 40$ and $278.15 \leq T \leq 308.15$ K are as follows:

$$\mathrm{pH_T} = \mathrm{p}(K_\mathrm{I}e_2) + \log\left(\frac{R - e_1}{1 - R\frac{e3}{e2}}\right)$$

where

$$e_1 = -0.007762 + 4.5174\mathrm{x}10^{-5}T$$

$$e_3/e_2 = -0.020813 + 2.60262 \times 10^{-4}T + 1.0436 \times 10^{-4}(S-35)$$

$$\begin{aligned}\mathrm{p}(K_\mathrm{I}e_2) = {} & 5.561224 - 0.547716S^{0.5} + 0.123791S - 0.0280156S^{1.5} + 0.00344940S^2 \\ & - 0.000167297S^{2.5} \\ & + 52.640726S^{0.5}T^{-1} + 815.984591T^{-1}\end{aligned}$$

This new model, appropriate for use with purified mCP, produces pH values that are within ± 0.004 of those obtained using previously published data and purified-mCP models for pure water and seawater.

1. Introduction

Spectrophotometric procedures remain largely underutilized for pH investigations of low-salinity waters ($S < 20$), although such methods are widely employed in open-ocean work (e.g., Robert-Baldo et al., 1985; Byrne et al., 1988; Byrne and Breland, 1989; King and Kester, 1989; Breland and Byrne, 1993; Clayton and Byrne, 1993; Liu et al., 2011). Because many important pH-dependent chemical processes occur in low-S environments such as lakes (e.g., Dean and Gorham, 1998; Alin and Johnson, 2007) and estuaries (e.g., Yao and Byrne, 2001; Feely et al., 2010; Hales et al., 2017), high-quality spectrophotometric pH measurements are essential for understanding the role of these environments in chemical cycling.

In the decades since the initial physical–chemical characterization of meta-cresol purple (mCP) for use in seawater (Clayton and Byrne, 1993), this sulfonephthalein dye has become the most widely used indicator for marine spectrophotometric pH measurements. Recently, mCP purification procedures (Liu et al., 2011; Patsavas et al., 2013; DeGrandpre et al., 2014; Lai et al., 2016, 2017) have alleviated earlier concerns about the effects of colorimetric impurities on measurement accuracy (Mosley et al., 2004; Yao et al., 2007; Douglas and Byrne, 2017). Efforts to employ spectrophotometric methods with a variety of

---

* Corresponding author at: 140 7th Avenue South, St. Petersburg, FL 33701, USA
E-mail address: rhbyrne@usf.edu (R.H. Byrne).

http://dx.doi.org/10.1016/j.marchem.2017.10.001
Received 28 September 2017; Accepted 11 October 2017

indicators in freshwater environments have included the works of Yao and Byrne (2001), French et al. (2002), Liu et al. (2006), Yuan and DeGrandpre (2008), and Lai et al. (2016, 2017). However, only two studies have been performed to allow for the use of mCP in estuaries (Mosley et al., 2004; Hammer et al., 2014), and both were conducted using unpurified mCP.

Mosley et al. (2004) used unpurified mCP to develop an S-dependent $\mathrm{p}K_\mathrm{I}$ relationship for mCP across the range $0 \le S \le 40$ at 298.15 K (where K_I is the dissociation constant of the indicator for the reaction $\mathrm{HL}^- \Leftrightarrow \mathrm{H}^+ + \mathrm{L}^{2-}$). Hammer et al. (2014) subsequently combined the S-dependent $\mathrm{p}K_\mathrm{I}$ of Mosley et al. (2004) and the T-dependent terms of Clayton and Byrne (1993) to create a model applicable to the Baltic Sea. However, the use of unpurified mCP can produce pH measurement errors on the order of 0.015 or larger (Douglas and Byrne, 2017). Such measurements can be corrected retrospectively to improve accuracy when original measurements are archived and a sample of the stock indicator is preserved (Douglas and Byrne, 2017), but a comprehensive, generally applicable model for purified mCP is preferable.

There are currently no characterizations of purified mCP over the wide range of S relevant to estuaries. Although $\mathrm{p}K_\mathrm{I}$ for purified mCP has recently been characterized at $S = 0$ over a range of T (Lai et al., 2016, 2017) the resulting measurement algorithm, which is based on the procedures of Yao and Byrne (2001), is subject to the limitations of the Davies (1962) equation for prediction of ion activity coefficients at ionic strengths substantially greater than zero (Millero and Schreiber, 1982). Consequently, a spectrophotometric pH measurement model is needed to facilitate the seamless use of mCP across aquatic and marine environments, from $S = 0$ to $S = 40$.

In the present work, using procedures similar to the pH-correction methods of Douglas and Byrne (2017), it is shown that previously determined $\mathrm{p}K_\mathrm{I}$ values for mCP (Mosley et al., 2004; $0 \le S \le 40$ at 298.15 K) can be corrected for the effects of indicator impurities. These corrected $\mathrm{p}K_\mathrm{I}$ values are then combined with the pH measurement algorithms for freshwater (Lai et al., 2016, 2017) and seawater (Liu et al., 2011) to produce a comprehensive and seamless model for mCP-based measurements of total proton scale pH ($\mathrm{pH_T}$) over the salinity range of 0 to 40 and the temperature range of 278.15 to 308.15 K.

Spectrophotometric pH of a water sample is determined using the following relationship (Byrne, 1987; Byrne and Breland, 1989; Clayton and Byrne, 1993):

$$\mathrm{pH_T} = \mathrm{p}K_\mathrm{I} + \log\left(\frac{R - e_1}{e_2 - Re_3}\right) \tag{1}$$

where $\mathrm{pH_T} = -\log\ [\mathrm{H}^+]_\mathrm{T}$, R is the ratio of the spectrophotometric absorbances (${}_{\lambda}A$) at the indicator's base-form (L^{2-}) and acid-form (HL^-) absorbance peaks ($R = {}_{578}A/{}_{434}A$), and the terms e_1, e_2, and e_3 (referred to generally as e_x) are HL^- and L^{2-} molar absorptivity ratios at selected wavelengths.

Liu et al. (2011) characterized the physical–chemical properties of HPLC-purified mCP in seawater and determined the T and S dependence of the e_x ratios and K_I. Their refined $\mathrm{pH_T}$ equation is given in the following form (Zhang and Byrne, 1996; Liu et al., 2011):

$$\mathrm{pH_T} = \mathrm{p}(K_\mathrm{I}e_2) + \log\left(\frac{R - e_1}{1 - R\frac{e_3}{e_2}}\right) \tag{2}$$

Additional information regarding the $\mathrm{p}(K_\mathrm{I}e_2)$, e_1, and e_3/e_2 terms can be found in Liu et al. (2011).

HPLC tests of off-the-shelf mCP have revealed that colorimetric impurities interfere with the absorbance of the HL^- peak at 434 nm, thus spuriously lowering the $\mathrm{pH_T}$ calculated from Eqs. (1) and (2) (Yao et al., 2007; Liu et al., 2011). With this observation in mind, Douglas and Byrne (2017) developed the following model to correct for absorbance contributions from impurities in commercially available mCP:

$$R_\mathrm{pure} = R_\mathrm{obs}\left(1 + \frac{{}_{434}A_\mathrm{imp}}{{}_{434}A_\mathrm{obs} - {}_{434}A_\mathrm{imp}}\right) \tag{3}$$

where R_pure is the R-ratio that would have been measured with purified mCP; R_obs is the R-ratio actually observed with unpurified mCP; ${}_{434}A_\mathrm{imp}$ is the 434 nm absorbance due to colorimetric impurities alone (experimentally determined for each lot of commercial mCP); and ${}_{434}A_\mathrm{obs}$ is the 434 nm sample absorbance observed using unpurified mCP. The ${}_{434}A_\mathrm{imp}$ term is determined by measuring absorbances of the unpurified mCP in solutions at high pH (~12), where the concentration of HL^- is negligible and all mCP is in the basic L^{2-} form. Measurements of absorbance ratios under these conditions can be used to reveal the small spectral influence of impurities in the presence of the dominant spectral signature of the L^{2-} species. The ${}_{434}A_\mathrm{imp}$ model assumes that any impurities in the dye solution do not participate in acid-base H^+ exchange equilibria and instead behave as inert chemical species in the sample; Douglas and Byrne (2017) found this assumption to be appropriate over the range $7.25 \le \mathrm{pH_T} \le 8.00$ for the six lots of unpurified mCP used to test the ${}_{434}A_\mathrm{imp}$ model (i.e., Eq. (3)).

In this work, the equations developed by Douglas and Byrne (2017) were extended to correct previously published experimentally determined $\mathrm{p}K_\mathrm{I}$ values for the effects of indicator impurities. The procedures developed for retrospective refinements of $\mathrm{p}K_\mathrm{I}$ values were then applied to the data set of Mosley et al. (2004).

2. Theory

Correction of previously published $\mathrm{p}K_\mathrm{I}$ values that were obtained using unpurified mCP can be performed using the following mathematical relationship for the spectral behavior of the indicator and the colorimetric impurities found in a dye solution: ${}_{434}A_\mathrm{obs} - {}_{434}A_\mathrm{mCP} = {}_{434}A_\mathrm{imp}$ (Eq. (7) of Douglas and Byrne (2017)).

Dividing Eq. (7) of Douglas and Byrne (2017) by ${}_{578}A$ results in the following expression:

$$\frac{{}_{434}A_\mathrm{obs}}{{}_{578}A} - \frac{{}_{434}A_\mathrm{mCP}}{{}_{578}A} = \frac{{}_{434}A_\mathrm{imp}}{{}_{578}A} \tag{4}$$

Eq. (4) can be rewritten as

$$(R_\mathrm{obs})^{-1} - (R_\mathrm{pure})^{-1} = \frac{{}_{434}A_\mathrm{imp}}{{}_{578}A} \tag{5}$$

From algebraic rearrangement of the fundamental equation that relates mCP absorbances to mCP molar absorptivities, dissociation constants, and pH (Eq. (5c) of Clayton and Byrne, 1993), ${}_{578}A$ can be expressed as follows:

$${}_{578}A = \left(\frac{{}_{578}\varepsilon_\mathrm{L} + {}_{578}\varepsilon_\mathrm{HL}\ K_\mathrm{I}^{-1}\ [\mathrm{H}^+]_\mathrm{T}}{1 + K_\mathrm{I}^{-1}\ [\mathrm{H}^+]_\mathrm{T}}\right) l\ [\mathrm{mCP}]_\mathrm{T} \tag{6}$$

where ${}_{578}\varepsilon_\mathrm{L}$ and ${}_{578}\varepsilon_\mathrm{HL}$ are the molar absorptivity coefficients for mCP at 578 nm for the L^{2-} and HL^- forms of mCP, respectively; $[\mathrm{H}^+]_\mathrm{T}$ is the total hydrogen ion concentration; l is the spectrophotometric cell pathlength; $[mCP]_\mathrm{T}$ is the total concentration of mCP; and K_I is the dissociation constant of mCP (equivalent to the inverse of the formation constant, which was used by Clayton and Byrne, 1993).

From the Beer-Lambert Law, ${}_{434}A_\mathrm{imp}$ is given as follows:

$${}_{434}A_\mathrm{imp} = ({}_{434}\varepsilon_\mathrm{imp})\ c\ l\ [\mathrm{mCP}]_\mathrm{T} \tag{7}$$

where ${}_{434}\varepsilon_\mathrm{imp}$ is the molar absorptivity coefficient of impurities and c is the constant of proportionality between the concentration of impurities and the concentration of mCP indicator in an unpurified dye solution. Combining Eqs. (6) and (7) and then rearranging, the term on the right side of Eq. (5) can be written as

$$\frac{{}_{434}A_\mathrm{imp}}{{}_{578}A} = \frac{\theta\ (1 + K_\mathrm{I}^{-1}\ [\mathrm{H}^+]_\mathrm{T})}{({}_{578}\varepsilon_\mathrm{L}/{}_{578}\varepsilon_\mathrm{HL}) + K_\mathrm{I}^{-1}\ [\mathrm{H}^+]_\mathrm{T}} \tag{8}$$

Table 1

Inputs (based on Table 2 of Mosley et al., 2004) and corresponding impurity-corrected outputs of R_{pure} and mCP pK_{I} values.

Inputs: from Mosley et al. (2004) data				Outputs: corrected values	
S	$\mathrm{pH_{tris}}$	$\mathrm{p}K_{\mathrm{I}}$	R_{obs}	R_{pure}	$\mathrm{p}K_{\mathrm{I}}$
0.06	8.0739	8.5626	0.697940	0.706456	8.5570
0.13	8.0737	8.5301	0.748921	0.758204	8.5244
0.27	8.0734	8.4849	0.825775	0.836251	8.4791
0.54	8.0728	8.4349	0.919031	0.931016	8.4289
1.01	8.0720	8.3803	1.031932	1.045833	8.3741
1.50	8.0712	8.3393	1.124683	1.140230	8.3329
2.00	8.0706	8.3069	1.203511	1.220509	8.3003
3.04	8.0694	8.2635	1.316040	1.335192	8.2567
4.03	8.0685	8.2305	1.408035	1.429021	8.2234
4.98	8.0677	8.2060	1.479686	1.502143	8.1988
7.51	8.0664	8.1556	1.638732	1.664600	8.1480
10.00	8.0660	8.1209	1.758759	1.787328	8.1130
14.99	8.0670	8.0738	1.940166	1.973030	8.0655
20.02	8.0706	8.0419	2.084332	2.125679	8.0321
20.26	8.0708	8.0425	2.082658	2.130824	8.0311
24.98	8.0763	8.0195	2.204901	2.230895	8.0136
30.01	8.0842	8.0094	2.285215	2.328938	7.9998
30.03	8.0842	8.0060	2.300660	2.329143	7.9998
35.02	8.0941	8.0013	2.367986	2.416186	7.9911
35.04	8.0941	7.9997	2.375464	2.416303	7.9910
39.99	8.1058	7.9975	2.441260	2.490691	7.9873
39.99	8.1058	7.9975	2.441260	2.490691	7.9873

where θ is defined as:

$$\theta = \frac{({}_{434}\varepsilon_{\mathrm{imp}})\, c}{{}_{578}\varepsilon_{\mathrm{HL}}} \tag{9}$$

Because the numerator of θ includes the molar absorptivity coefficient of impurities and depends on the proportionality constant c, values of θ are specific to every source of indicator, i.e., specific to a particular batch of synthesized mCP. If more than one dye source were used during the course of a series of measurements, more than one value of θ would be needed. Our work assumes that a single dye solution was used for the experiments of Mosley et al. (2004), and that one value of θ is sufficient for the impurity correction.

Finally, using the definitions of e_1 and e_2, Eqs. (5) and (8) can be combined to calculate R_{pure} from R_{obs}, the molar absorptivity ratios, and the known $[\mathrm{H}^+]_{\mathrm{T}}$ values of buffer solutions:

$$(R_{\mathrm{obs}})^{-1} - (R_{\mathrm{pure}})^{-1} = \frac{\theta\,(1 + K_{\mathrm{I}}^{-1}\,[\mathrm{H}^+]_{\mathrm{T}})}{{}^{e_2}\!/_{e_1} + K_{\mathrm{I}}^{-1}\,[\mathrm{H}^+]_{\mathrm{T}}} \tag{10}$$

Eq. (10) allows for the calculation of θ, an inherent characteristic of the unpurified indicator used by Mosley et al. (2004), from four known or calculable variables: (1) the K_{I} results of Mosley et al. (2004) at each measured $\mathrm{pH_{tris}}$ for samples with $20 \le S \le 40$; (2) the e_{x} values of Clayton and Byrne (1993), used by Mosley et al. (2004); (3) the Mosley et al. (2004) R_{obs} values and $\mathrm{pH_T}$ measurement algorithm; and (4) R_{pure} results calculated from the model of Liu et al. (2011), to correspond to the buffers (i.e., $[\mathrm{H}^+]_{\mathrm{T}}$ values) used by Mosley et al. (2004) within the range of conditions ($20 \le S \le 40$) relevant to the model of Liu et al. (2011).

Subsequently, using the average value of θ determined in these calculations, Eq. (10) can be used to provide R_{pure} values for each of the buffers used by Mosley et al. (2004). Finally, using these R_{pure} values in conjunction with the S- and T-dependent e_1 and e_3/e_2 equations of Liu et al. (2011), impurity-corrected values of $\mathrm{p}(K_{\mathrm{I}}e_2)$ can be determined (rederived) from the data of Mosley et al. (2004). These impurity-corrected values can then be combined with the algorithms for freshwater (Lai et al., 2016, 2017) and seawater (Liu et al., 2011) to provide a model that enables the use of mCP for pH measurements in waters of $0 \le S \le 40$ and $278.15 \le T \le 308.15$ K.

3. Methods

3.1. Obtaining impurity-corrected mCP $\mathrm{p}(K_{\mathrm{I}}e_2)$ values for $0 \le S \le 40$ at $T = 298.15$ K

Data inputs came from Table 2 of Mosley et al. (2004), reprinted here in Table 1. The pH of each tris buffer solution is given on the total pH scale (mol kg-soln^{-1}). All calculations were performed using the MATLAB 2014b software program.

The following procedure was used to calculate new $\mathrm{p}(K_{\mathrm{I}}e_2)$ values from the data of Mosley et al. (2004) for $0 \le S \le 40$ at $T = 298.15$ K:

1. Using Eq. (1), R_{obs} was calculated for each row of data in Table 1 (i.e., across all salinities). The $\mathrm{pH_{tris}}$ and $\mathrm{p}K_I$ data of Mosley et al. (2004) were used to calculate R_{obs}. Consistent with the original assumptions of Mosley et al. (2004), the molar absorptivity (e_x) ratios of Clayton and Byrne (1993) were used in these calculations: $e_1 = 0.00691$, $e_2 = 2.2220$, and $e_3 = 0.1331$.
2. For the subset of Table 1 data with $S \ge 20$, R_{pure} was calculated using Eq. (2). R_{pure} is the value that theoretically would have been obtained had Mosley et al. (2004) used purified mCP. For each sample with $S \ge 20$, values of $\mathrm{p}(K_{\mathrm{I}}e_2)$, e_1, and e_3/e_2 were calculated according to the equations of Liu et al. (2011). The $\mathrm{pH_{tris}}$ data in Table 2 of Mosley et al. (2004) were used.
3. Using Eq. (10) and calculated values of R_{obs} and R_{pure} for the subset of Table 1 data with $\mathrm{S} \ge 20$, θ values were calculated, and the mean value of θ (hereafter referred to as $\bar{\theta}$) was determined. For this calculation, K_{I} values (calculated from $\mathrm{p}K_I$ in Table 2 of Mosley et al., 2004), $[\mathrm{H}^+]_{\mathrm{T}}$ (calculated from $\mathrm{pH_{tris}}$ in Table 2 of Mosley et al., 2004), and the ratio $e_2/e_1 = 2.2220/0.00691 = 321.56295$ were used.
4. For the subset of Table 1 data with $S < 20$, Eq. (10) and $\bar{\theta}$ were used to calculate the quantity $(R_{\mathrm{obs}})^{-1} - (R_{\mathrm{pure}})^{-1}$, from which R_{pure} values could be calculated. For this calculation, $\bar{\theta}$ (from Step 3), K_{I} values (calculated from $\mathrm{p}K_I$ in Table 2 of Mosley et al., 2004), $[\mathrm{H}^+]_{\mathrm{T}}$ (calculated from $\mathrm{pH_{tris}}$ in Table 2 of Mosley et al., 2004), the ratio $e_2/e_1 = 321.56295$, and R_{obs} values (calculated in Step 1) were used.
5. For the entire range of salinity, Eq. (1) and the R_{pure} values (resulting from Steps 2 and 4) were used to calculate K_{I} and $\mathrm{p}K_{\mathrm{I}}$ values for each sample. The R_{pure} values used in this step were obtained from Step 4 for samples with $S < 20$ and in Step 2 for samples with $S \ge 20$. The $\mathrm{pH_{tris}}$ values from Table 2 of Mosley et al. (2004) and the e_x values of Clayton and Byrne (1993) were utilized in Eq. (1).
6. Steps 3–5 were repeated using the new K_{I} values for Steps 3 and 4. This procedure was performed iteratively until $\mathrm{p}K_{\mathrm{I}}$, $\bar{\theta}$, and R_{pure} no longer changed from one iteration to the next, i.e., no value changed by $> 10^{-6}$ between subsequent iterations. (Values stabilized after three iterations; typically $\bar{\theta} \approx 1.387$).
7. Using $e_2 = 2.2220$, the value assumed by Mosley et al. (2004), and the final $\mathrm{p}K_{\mathrm{I}}$ values from Step 6, new values of $\mathrm{p}(K_{\mathrm{I}}e_2)$ were determined.

3.2. Deriving a new model for $\mathrm{p}(K_{\mathrm{I}}e_2)$ across a range of S and T

In order to incorporate T dependence into our algorithm, the impurity-corrected $\mathrm{p}(K_{\mathrm{I}}e_2)$ values calculated in Step 7 above (based on the 298.15 K data of Mosley et al., 2004) were combined with the temperature-dependent freshwater model (Lai et al., 2016, 2017) and the salinity and temperature-dependent marine model (Liu et al., 2011). A best-fit algorithm for $\mathrm{p}(K_{\mathrm{I}}e_2)$ across the ranges $0 \le S \le 40$ and $278.15 \le T \le 308.15$ K was thereby determined as follows:

1. For $S = 0$ and $281.15 \le T \le 303.15$ K, values of e_2 and $\mathrm{p}K_{\mathrm{I}}$ were calculated using the equations found in Tables 2 and 3 of Lai et al. (2016, 2017) at temperature intervals of 2 K. These values of e_2 and

Table 2
Estuarine pH_T model and parameterizations for $0 \leq S \leq 40$ and $278.15 \leq T \leq 308.15$ K.

Model	Source	Equation	Test values ($S = 35$, $T = 298.15$ K, $R = 1$)
pH_T	Liu et al. (2011)	$pH_T = p(K_I e_2) + \log\left(\frac{R - e_1}{1 - R\frac{e_3}{e_2}}\right)$	7.66993
e_1	Liu et al. (2011)	$e_1 = -0.007762 + 4.5174 \times 10^{-5}T$	0.00571
e_3/e_2	Liu et al. (2011)	$\frac{e_3}{e_2} = -0.020813 + 2.60262 \times 10^{-4}T + 1.0436 \times 10^{-4}(S - 35)$	0.05678
$p(K_I e_2)$	This work	$p(K_I e_2) = 5.561224 - 0.547716\, S^{0.5} + 0.123791\, S - 0.0280156\, S^{1.5} + 0.00344940\, S^2 - 0.000167297\, S^{2.5} + 52.640726\, S^{0.5}\, T^{-1} + 815.984591\, T^{-1}$	7.64703

pK_I were then used to calculate $p(K_I e_2)$ values. Values of $p(K_I e_2)$ were then calculated as the difference of pK_I and $\log_{10}(e_2)$. The number of S–T combinations and corresponding $p(K_I e_2)$ values determined in this step (n_{Lai}) is 12.

2. For $20 \leq S \leq 40$ and $278.15 \leq T \leq 308.15$ K, values of $p(K_I e_2)$ were calculated according to the equations of Liu et al. (2011) at 4-unit salinity intervals and 5 K temperature intervals. The number of S–T combinations and corresponding $p(K_I e_2)$ values determined in this step (n_{Liu}) is 42.
3. These $p(K_I e_2)$ values were combined with the impurity-corrected $p(K_I e_2)$ values derived from the data of Mosley et al. (2004) (Table 1). The number of S–T combinations and corresponding $p(K_I e_2)$ values for the corrected Mosley data ($n_{Mosley,corr}$) is 22.
4. To ensure that all three data sets (each with a different number of data points) were given equal consideration in the multivariate polynomial fit for $p(K_I e_2)$, each $p(K_I e_2)$ value was assigned a weight, W_{source}, that was inversely proportional to the size of the source data set. W_{Lai} was arbitrarily assigned a value of 1, whereupon $W_{Liu} = 0.28571$ and $W_{Mosley,corr} = 0.54545$. For example, each $p(K_I e_2)$ value calculated using the model of Lai et al. (2016, 2017) was weighted by a factor of 3.5 relative to the $p(K_I e_2)$ values calculated using the Liu et al. (2011) model ($n_{Liu} = 3.5(n_{Lai})$).
5. A multivariate polynomial fit of the $p(K_I e_2)$ data was performed using the MATLAB *stepwiselm* tool, with $S^{0.5}$ and T^{-1} serving as the independent variables for fifth- and first-order polynomials (including an S-T interaction term) and the data were weighted according to Step 10 above. The full data set used for this fit is summarized in Appendix A. The *stepwiselm* tool generates a polynomial fit of the independent variables, up to the highest-order polynomial specified by the user, by adding or removing terms by stepwise regression, using F-test results to determine whether or not a term is added ($p \leq 0.05$ for the addition of a term) or removed ($p \geq 0.10$ for the removal of a term). This process continues until no more terms can be added or removed from the model, and the model is considered to be optimized.

4. Results

4.1. New $p(K_I e_2)$ model parameterization

The results of the R_{obs} calculations and the iterative calculations of R_{pure} and K_I (here reported as pK_I values) are shown in Table 1. The final values of R_{pure} are 0.009–0.049 higher than their corresponding R_{obs} values, consistent with the improvements that Douglas and Byrne (2017) obtained when applying the ${}_{434}A_{imp}$ correction to their absorbance data. The final corrected values of pK_I are 0.0056–0.0114 lower than the original results of Mosley et al. (2004). Smaller differences between the original (input) and impurity-corrected (output) pK_I values are generally observed at low salinities. This pattern is expected because the larger difference between pH_{tris} and pK_I at low ionic strength (with pH being less than pK_I) increases the HL^-/L^{2-} concentration ratio and thereby minimizes the influence of impurity absorption on the pH calculations (Douglas and Byrne, 2017). The new fit for $p(K_I e_2)$ as a function of S and T is given in Table 2 ($r^2 \geq 0.9999$), along with the e_x parameterizations (Liu et al., 2011) needed to calculate pH_T. Although the Liu et al. (2011) e_x parameterizations were obtained only over a marine salinity range, they are assumed to apply over the full estuarine range for the purposes of these calculations.

Residuals of $p(K_I e_2)$, expressed as differences between the $p(K_I e_2)$ characterizations derived from prior studies and the values calculated according to the new model (Table 2), are shown in Fig. 1 as a function of salinity, and the temperatures of the data are color coded. The new estuarine model fits the $p(K_I e_2)$ values within ± 0.004 across the full range of temperature and salinity conditions. The Mosley et al. (2004) dataset contained multiple samples at $S \sim 20$, 30, 35, and 40. Because the paired $p(K_I e_2)$ values at these salinities were in very close agreement, the paired residuals overlap and appear as only a single star at each salinity (Fig. 1).

4.2. Comparisons of pH_T within the freshwater and marine salinity ranges

Using the freshwater ($S = 0$) model of Lai et al. (2016, 2017) the marine ($20 \leq S \leq 40$) model of Liu et al. (2011), and the estuarine ($0 \leq S \leq 40$) model of this study (Table 2), pH_T values were calculated across each model's applicable ranges of S and T for R-ratios ranging between 0.2 and 2.0. The pH_T values calculated in this manner ranged from 6.8 to 8.8. The pH residuals, defined as $\Delta pH_T = pH_T$(Lai or Liu model) – pH_T(estuarine model), are identical to the $p(K_I e_2)$ residuals shown in Fig. 1 within ± 0.0006. Consequently, as for the $p(K_I e_2)$

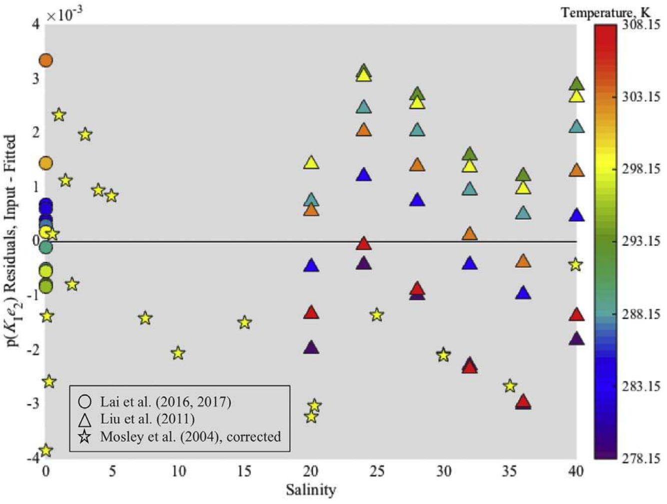

Fig. 1. Residuals for the new $pK_I e_2$ model (given in Table 2) as a function of salinity. Residuals are calculated as model input (as shown in the figure legend) minus the fitted values given by the new estuarine model. Colors represent temperature.

residuals, the pure and marine water pH_T residuals are within approximately ± 0.004, independent of the R-ratio. The residuals of pH_T and $p(K_Ie_2)$ are strongly correlated because the influence of variations in the modeled e_1 and e_3/e_2 terms (Eq. (2)) is comparatively small.

5. Discussion

This work provides, for the first time, a model appropriate for obtaining impurity-free spectrophotometric mCP-based pH measurements across the full range of river-to-sea salinities. The model described in Table 2 combines information from three independent studies of the molecular characteristics of mCP, including one that was herein corrected for the effects of indicator impurities. The new pH_T model agrees well with the empirical freshwater models of Lai et al. (2016, 2017) (approximately ± 0.003 for zero ionic strength and $281.15 \le T \le 303.15$ K), the empirical marine model of Liu et al. (2011) (approximately ± 0.003 pH units for $20 \le S \le 40$ and $278.15 \le T \le 308.15$ K), and the impurity-corrected estuarine data of Mosley et al. (2004) (approximately ± 0.004 for $0 \le S \le 40$ and $T = 298.15$ K). Given that different methodologies were used for these three different studies, we consider this agreement to be very good. The ± 0.004 internal consistency of the composite estuarine pH model should be sufficient to reliably monitor the often-large pH variability observed in estuarine environments (e.g., Mosley et al., 2004).

It is important to be aware that spectrophotometric pH measurements made in freshwater present challenges not encountered for measurements in seawater (Yao and Byrne, 2001). For example, adding mCP to a sample solution causes pH perturbations (Clayton and Byrne, 1993; Dickson et al., 2007; Lai et al., 2016) that are inversely proportional to the solution's buffer intensity (Stumm and Morgan, 1981). Because the total alkalinity of marine water is consistently on the order of ~2000 μM, the buffer intensity of seawater leads to relatively small indicator-induced pH perturbations. In freshwater, though, the alkalinity and buffer intensity are commonly much lower, so mCP perturbation effects are generally much larger.

To minimize this perturbation effect, the R of the indicator solution can be adjusted to match that of the sample solution as closely as possible by the addition of acid or base to raise or lower the indicator solution R-ratio. One can also apply a perturbation correction in which stepwise indicator additions are performed in order to linearly extrapolate observed pH values (or R values) to a pH appropriate to near-zero concentrations of mCP (Clayton and Byrne, 1993; Dickson et al., 2007; Lai et al., 2016). For very weakly buffered samples (e.g., fresh water), the use of a long-pathlength spectrophotometric cell (10 cm or longer) is recommended to minimize the amount of indicator required to be added (Yao and Byrne, 2001; Dickson et al., 2007; Yuan and DeGrandpre, 2008).

Such measures are important for improving the accuracy and precision of pH measurements, but the optimal precision or accuracy for a given undertaking should be assessed in the context of project aims and also of the temporal and spatial variability of the system under investigation. For example, accurate indicator-addition perturbation corrections are essential for rigorous measurements of open-ocean pH, where demands for precision on the order of 0.001 or better are standard. In a spatially heterogeneous system, however, where large pH variations (i.e., > 0.01 pH units) occur on a scale of several meters, pH precisions of ± 0.001 may be excessively burdensome and a pH perturbation correction may not be warranted. If accuracy better than ± 0.01 is desired, perturbation corrections are recommended (Lai et al., 2016), and likely essential.

Another matter of considerable concern for pH measurements at very low ionic strength is the large influence of salinity on pH measurement accuracy. For salinities between 0 and 1 at $T = 298.15$ K, the $p(K_Ie_2)$ of mCP changes by > 0.2. As such, accurate and precise salinity or ionic strength measurements are essential for making accurate and precise pH measurements at low ionic strength. Accurate pH measurements in freshwater at very low ionic strengths additionally require careful specification of the ionic composition of the measured medium. Freshwater generally lacks the constancy of composition of seawater (i.e., constant concentration ratios for major seawater ions). Therefore, conductivity measurements may not provide a highly reliable measure of ionic strength. The issue of composition constancy further complicates comparisons between measurements made on different pH scales (i.e., free versus total) at low ionic strengths. Additional useful discussion of this point can be found in Lai et al. (2016).

With the creation of the estuarine pH model, there are now two models appropriate for mCP pH measurements in fresh waters: Lai et al. (2016, 2017) and this work. There are also two models appropriate for measurements in marine systems, $S = 20$ to 40: Liu et al. (2011) and this work. For salinities between those conditions—i.e., the full range of estuarine conditions—this work fills an important gap. The new estuarine pH_T model is appropriate for both in situ measurements and the calibration of electrometric pH-measuring devices because it includes the influences of T and S over wide ranges.

Acknowledgments

The authors wish to thank Luke M. Mosley, Shamus L.G. Husheer, and Keith A. Hunter for their careful investigation of mCP characteristics, published as Mosley et al. (2004), and for the inclusion of their full data set in a form that can be used by others. The authors also thank Xuewu Liu, Mark C. Patsavas, Chun-Ze Lai, Michael D. DeGrandpre, Brandon D. Wasser, Taymee A. Brandon, Daniel S. Clucas, Emma J. Jaqueth, Zachary D. Benson, Corry M. Beatty, and Reggie S. Spaulding for their mCP characterizations, published as Liu et al. (2011) and Lai et al. (2016, 2017), which were used extensively throughout this work. Insightful and helpful editorial comments from Tonya Clayton are greatly appreciated. The comments of Michael DeGrandpre and one anonymous reviewer significantly improved our work. Special thanks is also given to Michael DeGrandpre for providing an advance copy of the corrigendum for the published work of Lai et al. (2016), cited throughout this document as Lai et al. (2017). This work was supported by the National Science Foundation, project numbers OCE 1220110 and OCE 1657894. N.K. Douglas was also supported by a Presidential Doctoral Fellowship from the University of South Florida Office of Graduate Studies.

Appendix A. Supplementary data

Supplementary data to this article can be found online at https://doi.org/10.1016/j.marchem.2017.10.001.

References

Alin, S.R., Johnson, T.C., 2007. Carbon cycling in large lakes of the world: a synthesis of production, burial, and lake-atmosphere exchange estimates. Glob. Biogeochem. Cycles 21 (3).

Breland, J.A., Byrne, R.H., 1993. Spectrophotometric procedures for determination of sea water alkalinity using bromocresol green. Deep-Sea Res. I Oceanogr. Res. Pap. 40 (3), 629–641.

Byrne, R.H., 1987. Standardization of standard buffers by visible spectrometry. Anal. Chem. 59, 1479–1481.

Byrne, R.H., Breland, J.A., 1989. High precision multi-wavelength pH determinations in seawater using cresol red. Deep-Sea Res. I 36, 803–810.

Byrne, R.H., Robert-Baldo, G., Thompson, S.W., Chen, C.T.A., 1988. Seawater pH measurements: an at-sea comparison of spectrophotometric and potentiometric methods. Deep Sea Res., Part A. 35 (8), 1405–1410.

Clayton, T.D., Byrne, R.H., 1993. Spectrophotometric seawater pH measurements: total hydrogen ion concentration scale calibration of *m*-cresol purple and at-sea results. Deep-Sea Res. I 40, 2115–2129.

Davies, C.W., 1962. Ion Association. Butterworths.

Dean, W.E., Gorham, E., 1998. Magnitude and significance of carbon burial in lakes, reservoirs, and peatlands. Geology 26 (6), 535–538.

DeGrandpre, M.D., Spaulding, R.S., Newton, J.O., Jaqueth, E.J., Hamblock, S.E., Umansky, A.A., Harris, K.E., 2014. Consideration for the measurement of spectrophotometric pH for ocean acidification and other studies. Limnol. Oceanogr. Methods

12, 830–839.

Dickson, A.G., Sabine, C.L., Christian, J.R. (Eds.), 2007. Guide to best practices for ocean CO_2 measurements. PICES Spec. Publ. 3.

Douglas, N.K., Byrne, R.H., 2017. Achieving accurate spectrophotometric pH measurements using unpurified meta-cresol purple. Mar. Chem. 190, 66–72.

Feely, R.A., Alin, S.R., Newton, J., Sabine, C.L., Warner, M., Devol, A., Krembs, C., Maloy, C., 2010. The combined effects of ocean acidification, mixing, and respiration on pH and carbonate saturation in an urbanized estuary. Estuar. Coast. Shelf Sci. 88 (4), 442–449.

French, C.R., Carr, J.J., Dougherty, E.M., Eidson, L.A.K., Reynolds, J.C., DeGrandpre, M.D., 2002. Spectrophotometric pH measurements of freshwater. Anal. Chim. Acta 453, 13–20.

Hales, B., Suhrbier, A., Waldbusser, G.G., Feely, R.A., Newton, J.A., 2017. The carbonate chemistry of the “fattening line,” Willapa Bay, 2011–2014. Estuar. Coasts 40 (1), 173–186.

Hammer, K., Schneider, B., Kulinski, K., Schulz-Bull, D.E., 2014. Precision and accuracy of spectrophotometric pH measurements at environmental conditions in the Baltic Sea. Estuar. Coast. Shelf Sci. 146, 24–32.

King, D.W., Kester, D.R., 1989. Determination of seawater pH from 1.5 to 8.5 using colorimetric indicators. Mar. Chem. 26, 5–20.

Lai, C.Z., DeGrandpre, M.D., Wasser, B.D., Branson, T.A., Clucas, D.S., Jaqueth, E.J., Benson, Z.D., Beatty, C.M., Spaulding, R.S., 2016. Spectrophotometric measurement of freshwater pH with purified meta-cresol purple and phenol red. Limnol. Oceanogr. Methods 14 (12), 864–873.

Lai, C.Z., DeGrandpre, M.D., Wasser, B.D., Branson, T.A., Clucas, D.S., Jaqueth, E.J., Benson, Z.D., Beatty, C.M., Spaulding, R.S., 2017. Corrigendum: Spectrophotometric measurement of freshwater pH with purified meta-cresol purple and phenol red. Limnol Oceanogr. Methods. http://dx.doi.org/10.1002/lom3.10210.

Liu, X., Wang, Z.A., Byrne, R.H., Kaltenbacher, E.A., Bernstein, R.E., 2006. Spectrophotometric measurements of pH in-situ: laboratory and field evaluations of instrumental performance. Environ. Sci. Technol. 40, 5036–5044.

Liu, X., Patsavas, M.C., Byrne, R.H., 2011. Purification and characterization of meta-cresol purple for spectrophotometric seawater pH measurements. Environ. Sci. Technol. 45, 4862–4868.

Millero, F.J., Schreiber, D.R., 1982. Use of the ion pairing model to estimate activity coefficients of the ionic components of natural waters. Am. J. Sci. 282 (9), 1508–1540.

Mosley, L.M., Husheer, S.L.G., Hunter, K.A., 2004. Spectrophotometric pH measurement in estuaries using thymol blue and m-cresol purple. Mar. Chem. 91, 175–186.

Patsavas, M.C., Byrne, R.H., Liu, X., 2013. Purification of meta-cresol purple and cresol red by flash chromatography: procedures for ensuring accurate spectrophotometric seawater pH measurements. Mar. Chem. 150, 19–24.

Robert-Baldo, G.L., Morris, M.J., Byrne, R.H., 1985. Spectrophotometric determination of seawater pH using phenol red. Anal. Chem. 57, 2564–2567.

Stumm, W., Morgan, J.J., 1981. Aquatic Chemistry. J. Wiley & Sons.

Yao, W., Byrne, R.H., 2001. Spectrophotometric determination of freshwater pH using bromocresol purple and phenol red. Environ. Sci. Technol. 35, 1197–1201.

Yao, W., Liu, X., Byrne, R.H., 2007. Impurities in indicators used for spectrophotometric seawater pH measurements: assessment and remedies. Mar. Chem. 107, 167–172.

Yuan, S., DeGrandpre, M.D., 2008. Evaluation of indicator-based pH measurements for freshwater over a wide range of buffer intensities. Environ. Sci. Technol. 42, 6092–6099.

Zhang, H., Byrne, R.H., 1996. Spectrophotometric pH measurements of surface seawater at in-situ conditions: absorbance and protonation behavior of thymol blue. Mar. Chem. 52, 17–25.